Supplement of Earth Syst. Dynam., 13, 1397–1415, 2022
https://doi.org/10.5194/esd-13-1397-2022-supplement
© Author(s) 2022. CC BY 4.0 License.

Earth System Dynamics
Open Access
EGU

Supplement of

An updated assessment of past and future warming over France based on a regional observational constraint

Aurélien Ribes et al.

Correspondence to: Aurélien Ribes (aurelien.ribes@meteo.fr)

The copyright of individual parts of the supplement might differ from the article licence.

1 Analysis of precipitation changes

1.1 Data

To characterize the past evolution of precipitation over Mainland France, the GPCC Full Data Monthly Product Version 2020 at 0.25° (GPCC hereafter) is used (Becker et al., 2013). Based on ∼85,000 rain gauges world-wide, GPCC provides gridded monthly land-surface precipitation from 1891–2019. Rain gauges data are quality-controlled before gridding but no homogenization procedure is applied. The rain-gauge density is quite heterogeneous from one region to the other, but relatively high over the selected Mainland France domain

In addition to GPCC, we use an observed dataset from Météo France (hereafter, MF). This dataset is based on monthly homogenized precipitation series, which are available for a large number of French measurement stations (more than 1000). They are obtained using the HOMER method (Mestre et al., 2013). The corresponding stations are not evenly distributed. To describe past evolution over Mainland France since 1958, a French index is obtained as an aggregation of these series in 3 steps. First, all monthly homogenized series available since 1958 are selected. Anomalies are computed as the ratio between monthly value and the monthly average value over the 1961-1990 period. Second, an aggregated anomaly is computed over each French department as the average of all the anomaly series in the department. Third, the French monthly anomaly series is the average of the monthly anomaly of each department weighted by its area.

1.2 Method

The statistical method used to investigate precipitation changes is close to that described in the main text. Regarding the estimation of the forced response in CMIP models, one noticeable difference is that we do not implement detection and attribution analysis, and so do not estimate the responses to NAT or GHG in CMIP6 models. The forced response (ALL) is estimated via a smoothing splines procedure with $df = 6$ equivalent degrees of freedom over the 1850–2100 period. There is no use of NAT-response EBM estimates in this case, so the possible response to the volcanic forcing is neglected. The remaining of the procedure is unchanged.

Then, we do not consider applying an observational constraint to precipitation for various reasons. Unlike for temperature, there is no reference showing a clear added-value of doing so with precipitation, homogenized observations are not available since the early 20th century, the signal-to-noise ratio of annual mean changes remains weak in many regions including France, and implementation would be technically challenging. Therefore, we only describe unconstrained model results in the following.

1.3 Results

A well-known feature of precipitation change is that the signal-to-noise (i.e., the magnitude of human-induced changes compared to natural internal variability) is much smaller than that of temperature

change. This is the reason why observations provide much less information about past and future changes in precipitation, if compared to temperature. As a result, we do not implement observational constraints for precipitation, and our analysis is primarily an assessment of raw CMIP6 results.

The time-series of observed precipitation and their forced response in CMIP6 simulations are shown in Figure S5 and S6.

Over the past (i.e., up to 2020), the forced response that is simulated by CMIP6 models remains very small for all seasons. The multi-model average exhibits an emerging but very limited winter increase and summer decrease over the last two decades. The magnitude of this change is about 5%, which is very small compared to year-to-year internal variability. Remarkably, the range of the CMIP6 forced response is also quite narrow. This suggests that models from this new CMIP6 generation exhibit stable pre-industrial control experiment, and that the forced response over the historical period can confidently be assessed as very limited.

The two observed datasets (GPCC and MF) agree pretty well over the last 60 year in terms of interannual variability. In order to better reflect long term changes in these observed records, a simple smoothing procedure is applied to raw data. This procedure is consistent with the way model data were processed, except that the smoothing parameter is adjusted to the length of the time-series. However, these smoothed observations are still not directly comparable to their simulated counterpart: most models have produced multiple historical simulations, which are averaged to improve estimation of the forced response, while only one observed time-series is available. After filtering, the two observed datasets exhibit no or very little change over the period 1958–2020. Observations are also consistent with CMIP6 models over this period (i.e., they stay well within the model simulated range for the forced response). Only over the period 1958–1970 and for annual precipitation, the filtered GPCC data are lower than the filtered MF data and CMIP6 models – but this is probably a side-effect of taking into account earlier years. Looking further back in time, the case is different. Prior to 1958, only the GPCC dataset is available, and it exhibits a clear positive trend (in winter and annual mean precipitation) that is larger than the forced response simulated by CMIP6 models. This discrepancy will require further research to be fully understood. Internal variability superimposed on the forced response could contribute to this trend. Observational issues related to poor spatial coverage or remaining inhomogeneities could also contribute to it – potentially questioning the credibility of GPCC observations over this early period. Alternatively, this discrepancy could be due to an underestimation of the simulated winter precipitation response to anthropogenic forcings across the 20th century, which would cast doubts on the model's ability to correctly project future changes in this season. Both the weak signal observed since 1958 and the lack of confidence in prior data led us to not applying observational constraint techniques to precipitation.

As for the future, CMIP6 projections are in line with previous assessments and multimodel ensembles such as CMIP5 (Terray and Boé, 2013). The response of annual mean precipitation is quite uncertain in sign, as some models simulate a decrease, while others simulate an increase. However, there is a slight tendency towards reduced precipitation in a very high emission SSP5-8.5 scenario, in the multi-model mean, and for a majority of models. The projected changes in this scenario ranges

from about -11% to +7% in the late 21st century (2070–2098 wrt 1971–2000, Figure S6), with a median estimate of -5%. The two versions of the CanESM5 model, which exhibit the highest wetting, make this a skewed distribution. Still, the expected change in annual mean precipitation is quite limited. The climate change signal is less ambiguous for other seasons. In winter, the CMIP6 models consistently point towards increased precipitation in the future. This applies to all periods and scenarios. The magnitude of the change in the very high emission SSP5-8.5 scenario is about +4% to +35% in the late 21st century (2070–2098 wrt 1971–2000, Figure S6). This change is reduced in the intermediate emission scenario SSP2-4.5. In summer, models also agree quite well and project declining rainfall. This signal is clearer in SSP5-8.5 rather than SSP2-4.5, as a small fraction of models simulate almost no change in the latter. The magnitude of the projected rainfall decrease ranges from -14% to -52% in the very high emission scenario SSP5-8.5 in the late 21st century (2070–2098 wrt 1971–2000, Figure S6), with the highest change approaching -60% in 2100. This suggests that very substantial changes cannot be ruled out.

Compared to the EURO-CORDEX and CMIP5 multi-model ensembles (Figure S6), seasonal changes are slightly more pronounced in CMIP6. In summer, the upper-bound is revised downward (i.e., becomes more negative) in CMIP6 compared to previous ensembles. This finding suggests that the hypothesis of no or limited summer drying can now be ruled out. In winter, the projected wetting is more pronounced in CMIP6 than in previous ensembles, particularly the upper bound. Lastly, CMIP6 results are consistent with previous ensembles in projecting a limited change in annual rainfall over France.

Like for regional temperature, changes in regional precipitation are found to be near-linear on the global mean warming (Figure S3) and on the cumulative CO_2 emissions since 1850 (Figure S4), although some influence from the aerosols is also discernible (aerosols tend to delay the regional response). Consequently, every tonne of CO_2 emissions is also expected to strengthen precipitation changes.

Overall, this descriptive analysis of the CMIP6 results provide a clear picture of wetter winters and dryer summers over France in the future compared to the recent climate. Changes in annual mean precipitation are expected to remain modest. The lack of clear observed trends make observational constraints ineffective for the moment. Then, there is a clear inconsistency between CMIP6 results and observations over the early 20th century, particularly pronounced in winter. Better understanding this discrepancy seems critical to get a comprehensive picture of past and future precipitation changes. This would require reexamining observations to determine whether the trend found over the first half of the 20th century is representative of a climate shift. It would also require large single model ensembles to better disentangle the forced precipitation response, and to better sample internal variability.

2 Supplementary Figures and Tables

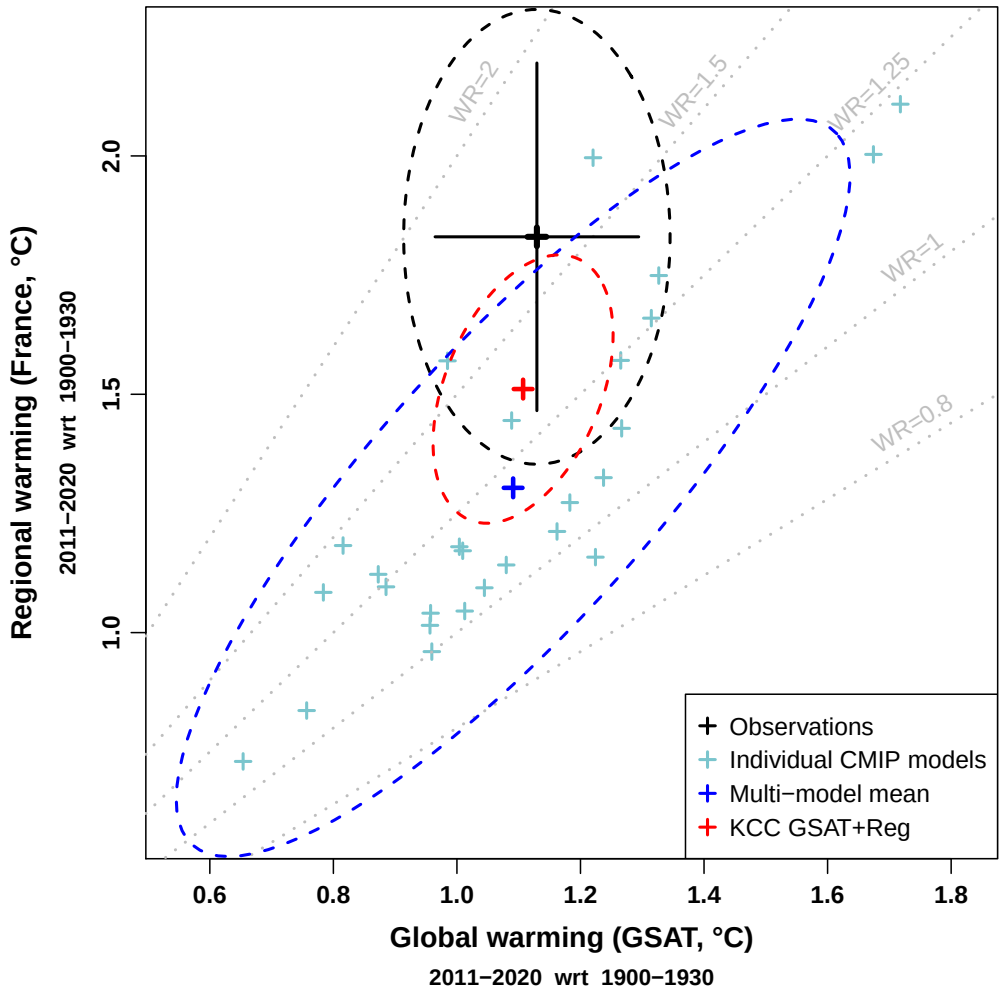

Figure S1: **Global to regional warming over the period 2011-2020.** Same as Figure 2 for the 2011-2020 period.

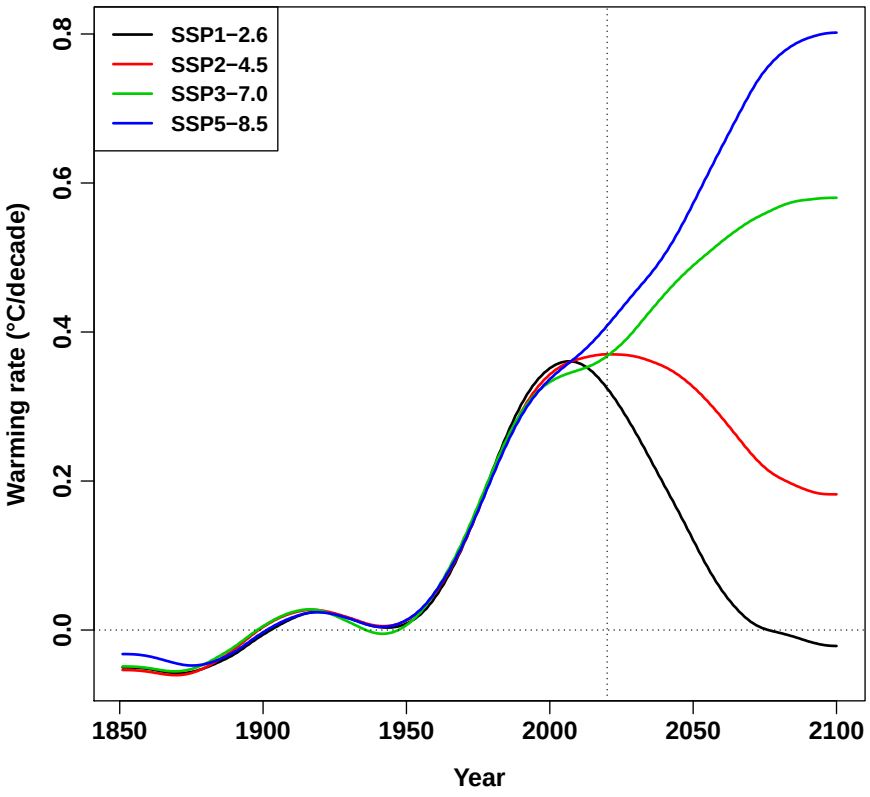

Figure S2: **Projected warming rate** (°C/decade) of human-induced warming after applying the observational constraint, for the 4 SSP scenarios considered. Dotted lines are indicative of no change (horizontal line), and the year 2020 (vertical line). Peak warming rate under the SSP2-4.5 scenario is found to occur exactly in 2020 over France.

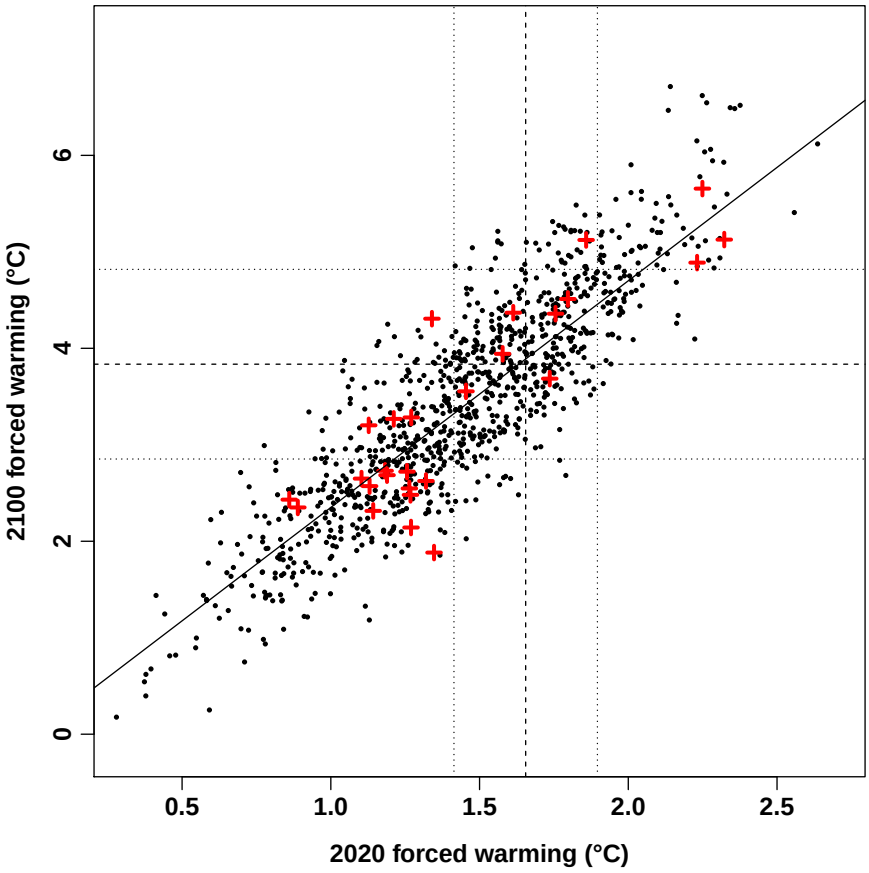

Figure S3: **Forced warming in 2100 vs 2020.** Near-linear relationship between the forced warming in 2020 and the forced warming in 2100 over France, in the ensemble of CMIP6 models (red crosses), and in our un-constrained prior distribution (black points; these points exhibits a correlation of 0.87). The vertical and horizontal lines correspond to the best-estimate (dashed line) and range (dotted lines) of our constrained estimates for the forced warming in 2020 and 2100, respectively. All results are for the intermediate emissions SSP2-4.5 scenario. The oblique solid line corresponds to a 2.4 ratio, suggesting that the 2100 forced warming is approximately 2.4 larger than the one in 2020.

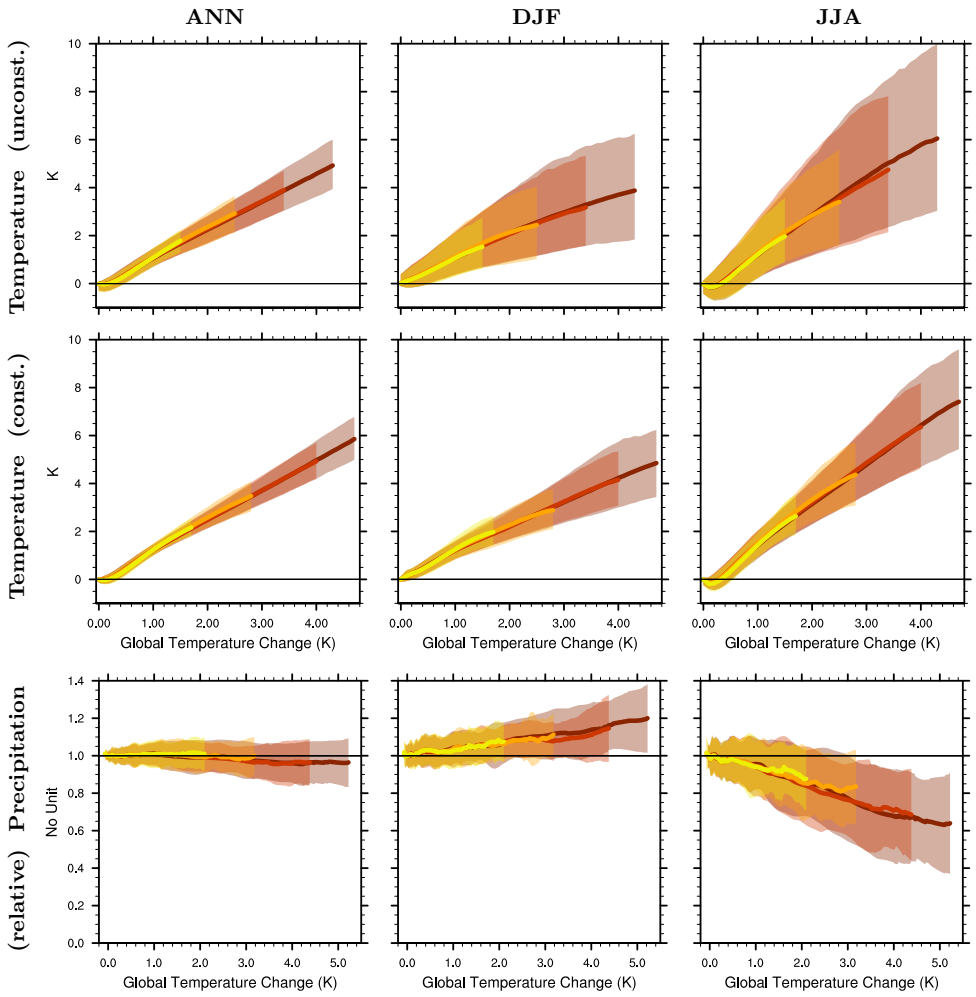

Figure S4: **Regional climate change vs global warming.** Regional climate change over France, as estimated for temperature (top and central rows) and precipitation (bottom row), in annual mean values (left column), winter (central column) and summer (right column), is compared to the global mean temperature change. The calculation for temperature is made for unconstrained projections (top row) as well as constrained projections (central row). Calculation is based on the four SSP scenarios used in this study: SSP1-2.6 (yellow), SSP2-4.5 (orange), SSP3-7.0 (red) and SSP5-8.5 (dark red). Regional changes are in general proportional to global mean warming, with some exception related to the influence of the aerosol forcing at low global warming (e.g., <1°C; more pronounced in summer).

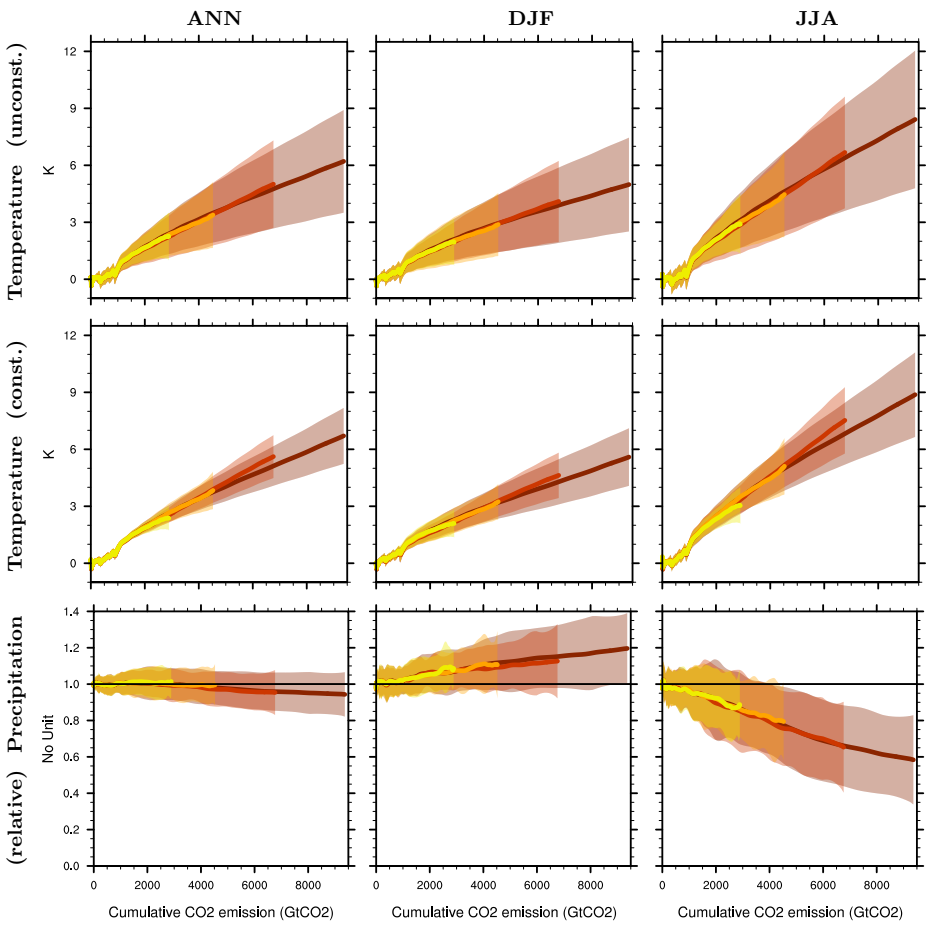

Figure S5: **Regional climate change vs cumulative CO_2 emissions.** Regional climate change over France as a function of cumulative CO_2 emissions since 1850. Results are shown for temperature (top and central rows) and precipitation (bottom row), in annual mean values (left column), winter (central column) and summer (right column). The calculation for temperature is made for unconstrained projections (top row) as well as constrained projections (central row). Calculation is based on the four SSP scenarios used in this study: SSP1-2.6 (yellow), SSP2-4.5 (orange), SSP3-7.0 (red) and SSP5-8.5 (dark red).

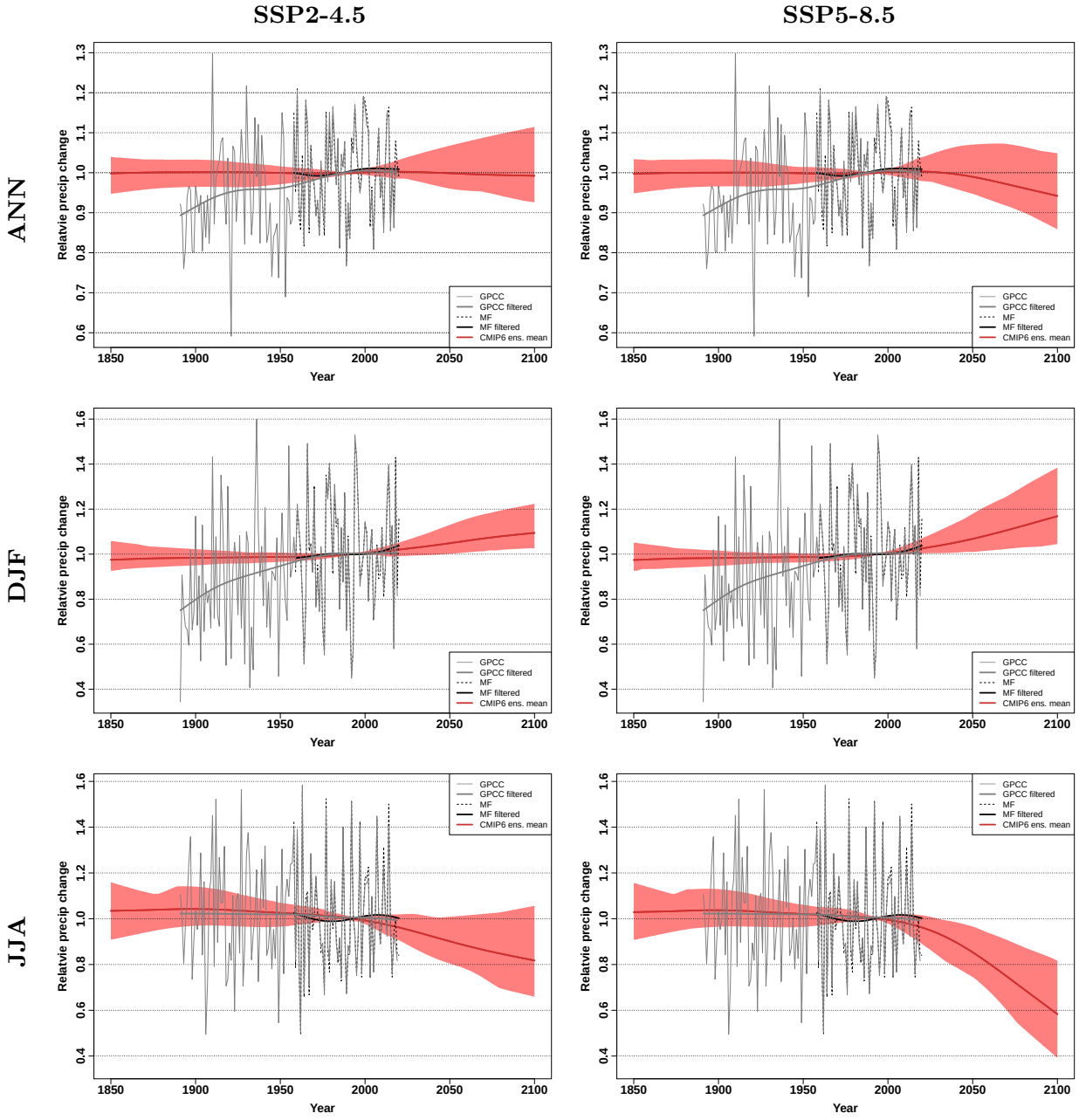

Figure S6: **Precipitation projections.** CMIP6 unconstrained projections for annual, winter and summer total precipitation over France, and for 2 illustrative SSP scenarios considered in this study. Observations from GPCC and MF (homogenized series post-1958) are compared to model outputs. These observed series are also filtered by applying a spline smoothing (with 4 and 3 degrees of freedom, respectively, to reflect the varying length of the records). The CMIP range is a 5 to 95% confidence range of the forced response, which is estimated from each CMIP6 model by applying a spline smoothing. Shown are relative anomalies with respect to the period 1959–2019 (i.e., the longest period covered by all 3 datasets).

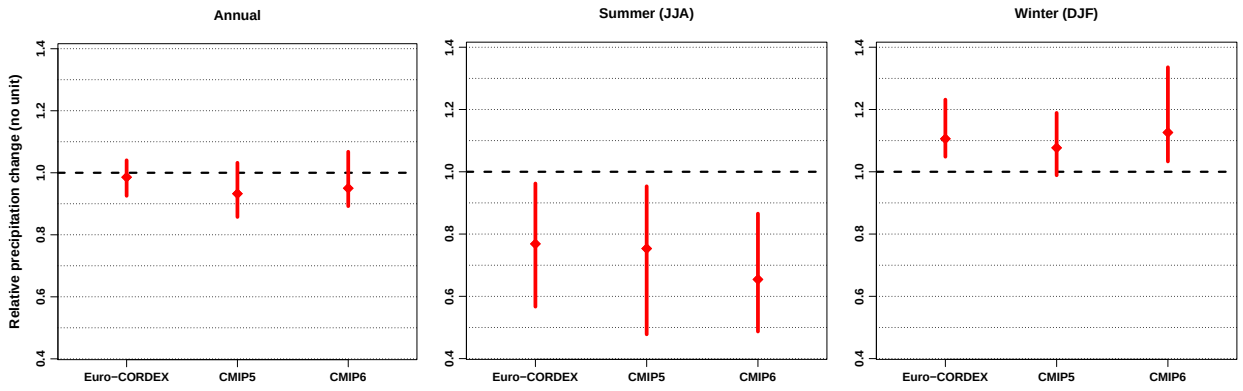

Figure S7: **Precipitation changes from various multi-model ensembles.** The relative change in annual, winter (DJF) or summer (JJA) mean precipitation, as estimated from the Euro-Cordex, CMIP5 and CMIP6 ensembles (all unconstrained). The comparison is made for the 2070–2098 vs 1971–2000 periods (covered by all model experiments), in the RCP8.5 (Euro-Cordex and CMIP5) or SSP5-8.5 (CMIP6) scenarios. All confidence ranges are 5-95% ranges, with the median used as a central estimate.

References

Becker, A., Finger, P., and Meyer-Christo, A.: A description of the global land-surface precipitation data products of the Global Precipitation Climatology Centre with sample applications including centennial (trend) analysis from 1901–present, p. 29, 2013.

Mestre, O., Domonkos, P., Picard, F., Auer, I., Robin, S., Lebarbier, E., Böhm, R., Aguilar, E., Guijarro, J., Vertachnik, G., and others: HOMER: a homogenization software – methods and applications, Id\Hojárás-Quarterly Journal of the Hungarian Meteorological Service, 117, 47–67, 2013.

Terray, L. and Boé, J.: Quantifying 21st-century France climate change and related uncertainties | Elsevier Enhanced Reader, https://doi.org/10.1016/j.crte.2013.02.003, 2013.